Advanced glycation end-products increase IL-6 and ICAM-1 expression via RAGE, MAPK and NF-κB pathways in human gingival fibroblasts

Kohei Nonaka[1], Yukari Kajiura[1], Mika Bando[1], Eijiro Sakamoto[1], Yuji Inagaki[1], Jung Hwan Lew[1], Koji Naruishi[1], Takahisa Ikuta[1], Kaya Yoshida[2], Tetsuo Kobayashi[3,4], Hiromasa Yoshie[4], Toshihiko Nagata[1], Jun-ichi Kido[1] *

1 Department of Periodontology and Endodontology, Institute of Biomedical Sciences, Tokushima University Graduate School, Tokushima, Japan.

2 Department of Oral Healthcare Education, Institute of Biomedical Sciences, Tokushima University Graduate School, Tokushima, Japan.

3 General Dentistry and Clinical Education Unit, Niigata University Medical and Dental Hospital, Niigata, Japan.

4 Division of Periodontology, Niigata University Graduate School of Medical and Dental Sciences, Niigata, Japan.

***Corresponding author:** Jun-ichi Kido
Department of Periodontology and Endodontology, Institute of Biomedical Sciences, Tokushima University Graduate School,
3-18-15 Kuramoto, Tokushima 770-8504, Japan
Phone: +81-88-633-7344; Fax: +81-88-633-7345
E-mail: kido.jun-ichi@tokushima-u.ac.jp

Running title: AGEs increase IL-6 and ICAM-1 expression

Keywords: AGE, IL-6, ICAM-1, human gingival fibroblasts

Number of figures and tables: 7 figures and 1 table.

Abstract

Background and Objectives: Diabetes mellitus (DM) is a risk factor for periodontal diseases and may exacerbate the progression of the pathogenesis of periodontitis. Advanced glycation end-products (AGEs) cause DM complications relative to levels of glycemic control and larger amounts accumulate in the periodontal tissues of patients with periodontitis and DM. In the present study, we investigated the effects of AGEs on the expression of inflammation-related factors in human gingival fibroblasts (HGFs) in order to elucidate the impact of AGEs on DM-associated periodontitis.

Materials and Methods: HGFs were cultured with or without AGEs. Cell viability was examined, and RNA and protein fractions were isolated from AGE-treated cells. The expression of IL-6, ICAM-1, and the receptor for AGE (RAGE) was investigated using RT-PCR, quantitative real-time PCR, and ELISA, and reactive oxygen species (ROS) activity was measured using a kit with 2',7'-dichlorofluorescin diacetate. Human monocytic cells (THP-1) labelled with a fluorescent reagent were co-cultured with HGFs treated with AGEs and IL-6 siRNA, and the adhesive activity of THP-1 cells to HGFs was assessed. The expression of IL-6 and ICAM-1 was examined when HGFs were pretreated with recombinant human IL-6 (rhIL-6), the siRNAs of RAGE and IL-6,

and inhibitors of MAPK and NF-κB, and then cultured with and without AGEs. The phosphorylation of MAPK and NF-κB was assessed using Western blotting.

Results: AGEs increased the mRNA and protein expressions of RAGE, IL-6, ICAM-1 and ROS activity in HGFs, and promoted the adhesion of THP-1 cells to HGFs, but had no effect on cell viability until 72 h. rhIL-6 increased ICAM-1 expression in HGFs, while the siRNAs of RAGE and IL-6 inhibited AGE-induced *IL6* and *ICAM1* mRNA expression, and IL-6 siRNA depressed AGE-induced THP-1 cell adhesion. AGEs increased the phosphorylation of p38 and ERK MAPKs, p65 NF-κB, and IκBα, while inhibitors of p38, ERK MAPKs, and NF-κB significantly decreased AGE-induced IL-6 and ICAM-1 expression.

Conclusions: AGEs increase IL-6 and ICAM-1 expression via the RAGE, MAPK and NF-κB pathways in HGFs and may exacerbate the progression of the pathogenesis of periodontal diseases.

Introduction

Diabetes mellitus (DM) is a major risk factor for periodontal diseases and the prevalence of periodontitis is higher in patients with DM than in individuals without DM (1,2). Epidemiological studies reported that clinical attachment loss and the risk of alveolar bone loss were greater in patients with uncontrolled DM than in individuals without DM (3,4) and periodontitis in patients with DM was sometimes associated with severe inflammation and the destruction of periodontal tissues (DM-associated periodontitis) (5-7). DM induces inflammatory responses in kidney, blood vessels, retina, and nerve tissues, and induces serious complications including nephropathy, neuropathy, and retinopathy, which exacerbate systemic conditions (8,9). Hyperglycemia occurs in DM and strongly induces the glycation of proteins via the non-enzymatic Maillard reaction, resulting in the production of advanced glycation end-products (AGEs) (10). AGEs bind to the receptor for AGE (RAGE) and increase the expression of pro-inflammatory cytokines such as IL-1β, IL-6, and TNF-α, enhance oxidative stress activity in some cells (11), cross-link extracellular matrix (ECM) proteins such as collagen and fibronectin, accumulate on the ECM, and weaken the structure of the ECM and bone (12).

AGEs accumulate in periodontal tissues in greater amounts in patients with DM than in individuals without DM (13) and are present in epithelial cells, fibroblasts, endothelial cells, and inflammatory cells in the periodontal tissues of patients with DM (14). RAGE is also known to be expressed in the gingival tissues of patients with DM (15), and RAGE mRNA expression in human gingival fibroblasts (HGFs) was previously shown to be increased by AGEs (16). AGEs inhibit collagen synthesis in HGFs (17), increase the expression of matrix metalloproteinase 1 (MMP-1) in HGFs (18), and decrease alkaline phosphatase activity and osteocalcin expression, but increase IL-1β expression in rat osteoblastic cells (19). These findings suggest that AGEs aggravate inflammation, the destruction of periodontal tissues, and bone resorption in DM-associated periodontitis.

Interleukin-6 (IL-6), a pro-inflammatory cytokine, is expressed in some cells including fibroblasts, epithelial cells, endothelial cells, osteoclasts, lymphocytes, and monocytes/macrophages, and influences inflammatory diseases including rheumatoid arthritis and periodontal diseases (20). IL-6 levels in the gingiva and peripheral blood were previously reported to be significantly higher in patients with periodontitis and type 2 DM than in patients with periodontitis, but without DM (21,22). When peripheral blood from patients with periodontitis and type 2 DM was stimulated with

Porphyromonas gingivalis (*P. gingivalis*)-lipopolysaccharide (*P.g*-LPS), IL-6 levels in blood increased more than in that from individuals without DM (22). Chiu *et al.* (23) recently showed that high glucose concentrations and AGEs as well as *P.g*-LPS increased IL-6 and IL-8 levels in HGFs. IL-6 is strongly expressed in periodontitis and DM and appears to play a role in the associated inflammatory responses.

Intercellular adhesion molecule-1 (ICAM-1) is a member of the immunoglobulin superfamily and is expressed on the membranes of some cells including endothelial cells, leukocytes, epithelial cells, and fibroblasts, and its levels are increased by bacterial pathogens and pro-inflammatory cytokines (24,25). ICAM-1 binds to lymphocyte function-associated antigen-1 (LFA-1) on leukocytes and monocytes, and functions in the adhesion and migration of these cells at inflammatory sites (25,26,27). *P.g*-LPS has been shown to increase ICAM-1 expression in the fibroblasts of gingival tissue with periodontal diseases, and soluble ICAM-1 serum levels were higher in periodontitis patients than in healthy individuals (28). *P. gingivalis* and *Aggregatibacter actinomycetemcomitans* (*A. actinomycetemcomitans*) increased the expression of ICAM-1 and IL-6 in human endothelial cells and gingival epithelial cells (29,30). On the other hand, plasma ICAM-1 levels were higher in patients with type 2 DM than in individuals with normal glucose tolerance (31), and AGEs increased the

gene expression of *ICAM1* and *RAGE* in human umbilical vein endothelial cells (32). These findings suggest that ICAM-1 is associated with the pathogenesis of periodontitis and DM.

In order to elucidate the mechanisms responsible for the DM-induced aggravation of periodontal diseases, we investigated the effects of AGEs on the expression of inflammation-related factors, particularly IL-6 and ICAM-1, in HGFs and also examined the AGE signaling pathway.

Materials and Methods

AGEs and reagents

AGEs were prepared according to the modified method of Takeuchi et al (33). Briefly, 50 mg/ml bovine serum albumin (BSA: Sigma-Aldrich; St. Luis, MO, USA) was mixed with DL-glyceraldehyde (0.1 M, Sigma-Aldrich), penicillin (100 U/ml), and streptomycin (100 μg/ml) in a sterile phosphate buffer (0.2 M, pH7.4) and incubated at 37°C for 7 days. The mixture was dialyzed against phosphate-buffered saline (PBS, pH7.4) to remove low-molecular-weight reactants and free glyceraldehyde. Non-glycated BSA as a control was prepared from the mixture without glyceraldehyde under the same conditions. AGE activity was assessed by the fluorescence of AGE

and non-glycated BSA solutions at excitation/emission wavelengths of 370/440 nm. The fluorescence of the AGE solution was 45-fold stronger than that of control non-glycated BSA. Dulbecco's Modified Eagle's Medium (DMEM), RPMI-1640 Medium, SB203580, and U0126 were obtained from Wako Pure Chemical Industries (Osaka, Japan) and fetal bovine serum (FBS) was from Biowest (Nuaillé, France). The Cell Explorer™ Fixable Live Cell Tracking Kit (Green Fluorescence) was from AAT Bioquest® (Sunnyvale, CA, USA). Recombinant human IL-6 (rhIL-6) was purchased from R&D systems (Minneapolis, MN, USA). SP600125 was from CALBIOCHEM (Darmstadt, Germany) and Bay11-7082 from Selleckchem (Houston, TX, USA). Antibodies against RAGE (#4679), p38 (phospho-p38 MAPK antibody: #4631, p38 antibody: #9212), ERK (phospho-p44/42 MAPK antibody: #4376, p44/42 MAPK antibody: #9102), JNK (phospho-SAPK/JNK antibody: #9251, SAPK/JNK antibody: #9252), p65 (phospho-NF-κB p65 antibody: #3033, NF-κB p65 antibody: #8242), IκBα (phospho-IκBα antibody: #2859, IκBα antibody: #4814), and horseradish peroxidase-conjugated goat anti-rabbit IgG were obtained from Cell Signaling Technology (Beverly, MA, USA). The β-actin antibody (#A2066) was obtained from Sigma-Aldrich.

Cell Culture

The HGF cell line CRL-2014® was obtained from ATCC (Manassas, VA, USA). HGFs were seeded at 4800 cells/cm^2 and cultured in DMEM supplemented with 10% FBS, penicillin, and streptomycin (growth medium) for five days and reached sub-confluency. HGFs were cultured with or without 50-1000 μg/ml of BSA or AGEs for 24-96 h and used in the cell proliferation assay, reverse transcription-polymerase chain reaction (RT-PCR), quantitative real-time PCR (qRT-PCR), Western blotting, ELISA, and ROS assay. In experiments using rhIL-6, sub-confluent HGFs were pre-cultured in DMEM-2% FBS for 24 h and then cultured with rhIL-6 (50 ng/ml) for 24 h (qRT-PCR) and 48 h (ELISA). In other experiment using MAPK and NF-κB inhibitors, HGFs were pre-cultured in DMEM-2% FBS for 24 h after sub-confluency and treated with MAPK inhibitors including SB203580 (30 μM), U0126 (10 μM), or SP600125 (10 μM) for 2 h or with an NF-κB inhibitor (Bay11-7082; 50 μM) for 24 h, and were then further cultured with 500 μg/ml BSA or AGEs for 24 h (qRT-PCR) and 48 h (ELISA). In assays on cell viability, ROS and cell adhesion, HGFs were seeded on a 96-welll plate (SUMITOMO BAKELITE, Tokyo, Japan) and 96-welll black plate (Thermo Scientific™ Nunclon™, Waltham, MA) at 4800 cells/m^2, cultured in DMEM supplemented with 10% FBS for 5 days, and then used for cell viability, ROS and cell

adhesion assays, respectively. THP-1 cells were cultured in RPMI-1640 medium containing 10% FBS and antibiotics and then used in cell adhesion assays with HGFs.

Cell viability assay

After sub-confluency, cell proliferation activity was examined using Cell Counting Kit-8 (CCK-8, DOJINDO, Kumamoto, Japan) according to the manufacturer's instructions. Briefly, cells were cultured with 500 μg/ml BSA or AGEs for 24, 48, 72, and 96 h, and were then incubated with 10 μl CCK-8 solution at 37°C for 2 h under a moist atmosphere with 5 % CO_2. The absorbance of each well was measured at 450 nm using a microplate reader (iMark™, Bio-Rad, Hercules, CA). The morphologies of cells treated with AGEs and BSA were observed using a phase contrast microscope at 40-fold magnification.

RT-PCR and quantitative real-time PCR

Total RNA was isolated from treated cells using the RNeasy® Mini Kit (QIAGEN, Hilden, Germany) and used for cDNA synthesis using the PrimeScript® II 1st strand cDNA Synthesis Kit (TaKaRa Bio, Otsu, Japan) according to the manufacturer's instructions. In RT-PCR, cDNA was added to the PCR mixture containing each primer

(Table 1), dNTPs, TaKaRa Taq™ HS, and PCR buffer (TaKaRa Bio). The PCR mixture was amplified for 34-40 cycles under the following conditions: denaturing at 94°C for 1 min, annealing at 55-60°C for 1 min, and extension at 72°C for 1 min. PCR products were analyzed by electrophoresis on a 1.5% agarose gel containing 0.1 μg/ml ethidium bromide. The expression of genes including *RAGE*, *IL6, ICAM1, MCP1, VEGF* (vascular endothelial growth factor), and *GAPDH* (glyceraldehyde 3-phosphate dehydrogenase) was investigated by RT-PCR. In qRT-PCR, the cDNA of IL-6, ICAM-1, or GAPDH was added to the PCR mixture containing primers (Table 1) and SYBR Green Supermix® (Bio-Rad, Hercules, CA, USA). The reaction was performed at 95°C for 30 s once, at 95°C for 5 s for 40 cycles, and at 60°C for 30 s using the CFX96™ Real-Time PCR Detection System (Bio-Rad). The relative mRNA levels of *IL6* and *ICAM1* were normalized to *GAPDH* mRNA.

Western blotting

HGFs were cultured with 500 μg/ml BSA or AGEs for 30 min (MAPK and NF-κB phosphorylation assays) and 24 h (RAGE western blot analysis), and cell lysates were extracted in lysis buffer including 10 mM Tris-HCl, pH 7.4, 50 mM NaCl, 5 mM EDTA, 1 mM sodium orthovanadate, 1 % NP-40, and protease inhibitor cocktail (Complete™;

Roche Diagnosis, Berkeley, CA). Total protein (10 μg) was electrophoretically separated on a denaturing 10 % polyacrylamide gel and transferred to a polyvinylidene difluoride membrane (Amersham Hybond-P: GE Healthcare Life Sciences, Buckinghamshire, UK). The membrane was blocked with PVDF Blocking Reagent for CanGet Signal® (TOYOBO, Osaka, Japan) at room temperature for 1.5 h and proteins on the membrane were reacted with rabbit antibodies (1/1000 dilution) against RAGE, p38 and phospho-p38, p44/42 (ERK) and phospho-ERK, SAPK/JNK (JNK) and phospho-JNK, p65- and phospho-p65, and IκBα and phospho-IκBα, and with a β-actin rabbit antibody (1/10000 dilution) at 4°C overnight, and then reacted with horseradish peroxidase-conjugated goat anti-rabbit IgG (Cell Signaling) at room temperature for 1.5 h. The reacted membrane was developed using ECL Western Blotting Detection Reagents (GE Healthcare Life Sciences) and exposed to Hyperfilm-ECL (GE Healthcare).

ELISA

The conditioned medium (supernatant) and cell lysate were collected from the culture of HGFs treated with AGEs or BSA for 48 h in order to examine the effects of AGEs on the production of IL-6 and ICAM-1. The supernatant was mixed with protease

inhibitor cocktail and cell lysates were extracted with a lysis buffer including 10 mM Tris-HCl, pH 7.4, 50 mM NaCl, 5 mM EDTA, 1 mM sodium orthovanadate, 1 % NP-40, and protease inhibitor cocktail. IL-6 in the supernatant was measured using the Human IL-6 ELISA kit (R&D Systems, Minneapolis, MN, USA) according to the manufacturer's instructions. ICAM-1 in cell lysates was determined using the Human ICAM1 ELISA kit (Biosensis, Thebarton, Australia). Total protein amounts in cell lysates were measured using the Bio-Rad protein assay reagent (Bio-Rad) and ICAM-1 levels were normalized to the total cell protein concentration.

Reactive oxygen species (ROS) measurement

Intracellular ROS levels were measured using the OxiSelect^{TM} Intracellular ROS Assay kit (Cell Biolabs, San Diego, CA). Briefly, HGFs were cultured in a 96-well black plate for 5 days and further incubated with 2', 7'-dichlorofluorescin diacetate (DCFH-DA, 20μM) at 37°C for 1 h. After cell washing with PBS, cells were stimulated with 500 μg/ml of BSA or AGEs for 6-72 h. DCFH-DA that diffused into cells was de-acetylated by cellular esterases to non-fluorescent 2'7'-dichlorofluorescein (DCF), the fluorescence of which shows the ROS level in a cell sample. Fluorescent was assessed at 480 nm/530 nm using the Varioskan^{TM} Flash Multimode Reader

(Thermo Scientific™, Waltham, MA).

Transfection of RAGE and IL-6 siRNAs

HGFs were seeded at 9500 cells/cm^2 and cultured in DMEM supplemented with 10% FBS to approximately 70% confluency. Medium was changed to DMEM with 2% FBS, and HGFs were then transfected with RAGE siRNA (10μM, BIONEER, Daejeon, Korea), IL-6 siRNA (10μM, Sigma-Aldrich), or control siRNA (10μM, Sigma-Aldrich) dissolved in Opti-MEM Medium (Invitrogen, Carlsbad, CA, USA) and Lipofectamine® RNA iMAX Reagent (Invitrogen) according to the manufacturer's instructions. After a 24 h culture, cells were treated with 500 μg/ml BSA or AGE for 48 h. Total RNA was extracted from cells transfected with each siRNA, and *RAGE* mRNA expression was confirmed by RT-PCR, and the expression of *IL6* and *ICAM1* mRNAs was investigated by qRT-PCR.

Cell adhesion assay

THP-1 cells were seeded at 1.5 x 10^6 cells/ml in culture medium and labelled with the Cell Explorer™ Fixable Live Cell Tracking Kit (Green Fluorescence) for cell adhesion assay according to the manufacturer's instruction. Briefly, a cell suspension was

mixed with an equal volume of the fluorescent reagent and incubated for 30 min in a CO_2 incubator. After washing in PBS three times, labelled THP-1 cells were added to HGFs treated with AGEs or IL-6 siRNA and then co-cultured for 30 min. Cells were washed with PBS three times to remove unattached THP-1 cells and observed using an inverted fluorescence microscope (ECLIPSE Ti-U, Nikon, Tokyo, Japan) at Ex/Em=490/520 nm and its NIS-Elements software (Nikon). The fluorescence intensity of labeled THP-1 cells that attached to HGFs was measured using a fluorescence microplate reader (TECAN Infinite® M200Pro, TECAN, Seestrasse, Switzerland) at Ex/Em=490/520 nm. In experiments of HGFs transfected with IL-6 siRNA, HGFs were transfected with IL-6 siRNA (10 μM, Sigma-Aldrich) or control siRNA (10 μM) and then treated with AGEs (500 μg/ml) and BSA for 24 h. The fluorescence intensity of labeled THP-1 cells that adhered to the treated HGFs was assessed using a fluorescence microplate reader. Cell adhesive activity was normalized to that of untreated (control) HGFs or HGFs treated with BSA.

Statistical analysis

All statistical analyses were performed with SPSS Statistics version 20 (IBM, Chicago, IL). The significance of differences between two groups was analyzed by the

Student's *t*-test. Comparisons of multiple groups were performed using a one-way analysis of variance (ANOVA) followed by Tukey's HSD. *P* values less than 0.05 were considered to be significant.

Results

AGEs do not affect the cell viability and morphology of HGFs cultured for 72 h

AGEs (500 μg/ml) did not affect the cell viability of HGFs by 72 h (Fig. 1A); however, cell viability significantly decreased by 96 h under culture conditions with AGEs (500 μg/ml) and BSA (500 μg/ml). AGEs did not affect cellular morphology when cells were cultured with AGEs and BSA (500 μg/ml each) for 72 h (Fig. 1B).

AGEs increase the expressions of RAGE, IL-6, ICAM-1 and ROS activity

AGEs (500 μg/ml) increased the mRNA expression of *RAGE*, *IL6* and *ICAM1* for 24-48 h, but did not markedly affect that of *MCP1* and *VEGF* by 72 h when the mRNA expression of factors was investigated by RT-PCR (Fig. 2A). AGEs dose-dependently (0-500 μg/ml) increased the mRNA expression of IL6 to approximately 2-fold that of the control (Fig. 2B) in the qRT-PCR assay, and 500 μg/ml of AGEs significantly increased the mRNA expression of *ICAM1* by approximately 3-fold (Fig. 2C).

AGEs (500 μg/ml) increased RAGE production in HGFs more than BSA for 24 h (Fig. 3A). When HGFs were cultured with AGE (500 μg/ml) and BSA for 48 h, the production of IL-6 and ICAM-1 was significantly up-regulated by approximately 2-fold and 3-fold, respectively (Fig. 3B and 3C). Furthermore, AGEs (500 μg/ml) significantly increased ROS activity in HGFs at 6 h in a time-dependent manner, and this activity was approximately 3-fold that of the control at 72 h (Fig. 3D).

IL-6 increases ICAM-1 expression and RAGE and IL-6 siRNAs inhibit AGE-induced *IL6* and *ICAM1* expression in HGFs

In order to investigate the mechanisms underlying AGE-induced IL-6 and ICAM-1 expression, HGFs were cultured with rhIL-6 (50 ng/ml) for 24 h (qRT-PCR) and 48 h (ELISA). rhIL-6 significantly increased the mRNA expression of *ICAM1* by 1.9-fold that of the control (Fig. 4A) and the expression of ICAM-1 protein by approximately 3-fold (rhIL-6: 1.58 ng/mg total protein) that of the control (0.52 ng/mg total protein) (Fig. 4B).

When HGFs were cultured with RAGE siRNA and then with AGEs, *RAGE* mRNA expression was inhibited (Fig. 4C) and AGE-induced *IL6* and *ICAM1* expression was significantly decreased by the knockdown of RAGE (Fig. 4D and 4E). IL-6

siRNA down-regulated the expression of *IL6* in HGFs stimulated by AGEs and BSA (Fig. 4F) and significantly decreased AGE-induced *ICAM1* expression to lower levels than that induced by BSA (Fig. 4G).

AGEs up-regulate IL-6 and ICAM-1 expression via MAPK and NF-κB pathways

The involvement of the MAPK pathway in AGE-induced IL-6 and ICAM-1 expression were investigated. When HGFs were stimulated by AGEs, the phosphorylation of p38 and ERK MAPK in cells was enhanced by AGEs, whereas that of JNK was not (Fig. 5A). AGEs increased the expression of *IL6* mRNA and the IL-6 protein in HGFs, and a p38 inhibitor (SB203580) and ERK inhibitor (U0126) significantly inhibited AGE-induced IL-6 expression at the mRNA and protein levels (Fig. 5B and 5D). However, a JNK inhibitor (SP600125) did not exert a significant inhibitory effect on AGE-induced IL-6 expression (mRNA and protein). In the expression of ICAM-1, SB203580 (p38 inhibitor) and U0126 (ERK inhibitor) clearly inhibited the AGE-induced expression of *IACM1* mRNA and the ICAM-1 protein, whereas SP600125 (JNK inhibitor) had no effect (Fig. 5C and 5E).

When the involvement of NF-κB in AGE-induced IL-6 and ICAM-1 expression was investigated, AGEs were found to increase the phosphorylation of p65 and IκBα

more than BSA (Fig. 6A). Bay11-7082 (NF-κB inhibitor) significantly decreased AGE- induced IL-6 expression at the mRNA and protein levels (Fig. 6B and 6D). The NF-κB inhibitor also significantly down-regulated the expressions of *ICAM1* mRNA and the ICAM-1 protein in HGFs stimulated by AGEs (Fig. 6C and 6E). These results showed that the p38, ERK MAPK and NF-κB pathways are involved in AGE-induced IL-6 and ICAM-1 expression in HGFs.

AGEs increase the adhesion of THP-1 cells to HGFs and IL-6 siRNA inhibits AGE-induced cell adhesion

THP-1 cells adhered to HGFs when both cells were co-cultured and the adhesion of THP-1 cells was increased by AGEs (Fig. 7A). AGEs (500 μg/ml) significantly up-regulated THP-1 cell adhesion to HGFs by approximately 1.4-fold that of BSA (Fig. 7B). The adhesion of THP-1 cells to HGFs significantly decreased when *IL6* expression in HGFs was inhibited by IL-6 siRNA and their adhesive level was approximately 58% that of AGE-stimulated adhesion (Fig. 7C).

Discussion

AGEs induce increases in inflammation and up-regulation of tissue degradation in

patients with DM resulting in end-organ complications such as microvascular diseases, nephropathy, neuropathy and retinopathy (8). AGEs increase the expression of pro-inflammatory cytokines such as IL-1β, IL-6, and TNF-α in some tissues (11) and inhibit collagen synthesis in gingival fibroblasts (17). Sakamoto et al. (19) reported that AGEs increased IL-1β expression and decreased bone nodule formation, alkaline phosphatase activity, and osteocalcin production in osteoblastic cells from rat bone marrow. AGEs and *P. gingivalis*-LPS exposure further increased IL-1β expression in osteoblastic cells (19). AGEs and the pathogens of periodontitis are considered to aggravate inflammation and degrade periodontal tissues in patients with periodontitis and DM.

IL-6 levels were previously reported to be high in the periodontal tissues and gingival crevicular fluid of patients with periodontitis (34,35). IL-1β and IL-6 levels in periodontal tissues were higher in patients with periodontitis and DM than in those with periodontitis, but not DM (21). IL-6 promotes the progression of periodontitis by inducing the expressions of proMMP-1, VEGF, and cathepsins in HGFs (36) and MMP-1 in human macrophages (37) as well as osteoclast formation (38). Sundararaji et al. (37) reported that a high glucose concentration (25 mM) increased IL-6 secretion from HGFs, and IL-6 levels from HGFs cultured in medium with high glucose

concentrations and LPS were higher than those in medium with high glucose concentrations, but no LPS. AGEs are known to accumulate at greater amounts in the gingival tissues of DM patients than in those of individuals without DM (13). The combination of high glucose concentrations and AGEs more strongly up-regulated IL-6 production, while the combination of AGEs and *P.g*-LPS under high glucose conditions synergistically increased IL-8 expression in HGFs (23). In the present study, AGEs increased IL-6 expression in HGFs and promoted the production of IL-6 and ROS activity in combination with *P.g*-LPS (data not shown). In addition, the combination of AGEs and *P.g*-LPS further increased the expression of inflammation-related factors and inhibited the differentiation of osteoblastic cells (19). These findings suggest that high glucose concentrations and AGEs induce inflammation in periodontal tissues by up-regulating IL-1β, IL-6 and IL-8 expression in DM, and the combination of *P.g*-LPS, hyperglycemia and AGEs may induce severe DM-associated periodontitis.

ICAM-1 influences the conditions of periodontitis and DM through its functions such as intercellular adhesion, migration, and immunological actions in leukocytes, endothelial cells, fibroblasts, and monocytes/macrophages (25,27-29,31). The expression of ICAM-1 is up-regulated by pro-inflammatory cytokines, and periodontopathic bacteria and their LPS in gingival fibroblasts, gingival epithelial cells,

and endothelial cells (28-30). In the present study, AGEs up-regulated the expression of RAGE, IL-6, and ICAM-1 in HGFs, and this was similar to the findings reported by Matsui showing that AGEs increased RAGE and ICAM-1 expression in umbilical vein endothelial cells (32). HGFs express ICAM-1 and THP-1 cells express LFA-1, which binds to ICAM-1 (39) and adheres to synovial fibroblasts (27). AGEs may recruit inflammatory cells to sites of periodontitis because AGEs increased an adhesive activity of monocytes (THP-1 cells) to HGFs in the present study. Furthermore, AGEs appear to influence inflammation in periodontitis and DM by binding to RAGE and regulating IL-6 and ICAM-1 expression in some cells in periodontal tissues because the knockdown of IL-6 in HGFs inhibited AGE-induced monocyte adhesion to HGFs.

Although AGEs up-regulated IL-6 and ICAM-1 expression in HGFs, the relationship between IL-6 and ICAM-1 expression currently remains unclear. IL-6 did not stimulate ICAM-1 expression in rat mesangial cells (40). In contrast, IL-6 induced ICAM-1 expression in human intestinal epithelial cells by activating NF-κB (41), and ICAM-1 expression in human synovial cells was increased by IL-6 and the soluble IL-6 receptor (sIL-6R), while an anti-ICAM-1 antibody suppressed IL-6-induced-osteoclastogenesis in RAW cells co-cultured with synovial cells (42). We investigated the effects of IL-6 on ICAM-1 expression when HGFs were cultured with rhIL-6, and

rhIL-6 significantly increased the expression of *ICAM1* mRNA (by approximately 2-fold of the control) and the ICAM-1 protein (by 3-fold of the control) in HGFs. Furthermore, the AGE-induced up-regulation of ICAM-1 and adhesion of THP-1 cells to HGFs were significantly inhibited by siRNA for IL-6, suggesting that AGEs increase ICAM-1 expression by up-regulating of IL-6 in HGFs and may exacerbate inflammation in periodontal tissues.

In the present study, AGEs increased the levels of ROS as well as IL-6 and ICAM-1 in HGFs. ROS damage periodontal tissues by degrading ECM proteins, inducing alveolar bone loss, and aggravating periodontal tissue destruction in periodontitis (43,44). AGEs increased plasminogen activator inhibitor-1 levels via ROS and the ERK and NF-κB pathways in human glomerular mesangial cells (45), up-regulated RAGE protein and intracellular ROS levels through ERK activation, induced mitogenesis in renal fibroblasts (46), and consequently influenced the pathogenesis of diabetic nephropathy. We speculate that AGEs exacerbate the progression of DM- associated periodontitis by stimulating inflammatory cytokines and ROS in gingival fibroblasts.

AGEs bind to RAGE on endothelial cells, epithelial cells, and fibroblasts in periodontal tissues (15,16), and RAGE is known to be strongly expressed in the gingiva

of patients with DM and periodontitis (47). AGEs induced MMP-1 expression via RAGE and NF-κB in fibroblasts isolated from human gingival tissues (18), and also increased IL-6, MCP-1, and VCAM-1 expression and stimulated migration capacity via the ERK, JNK, p38 MAPK, and NF-κB pathways in adventitial fibroblasts (48). AGE-induced collagen synthesis in cardiac fibroblasts was down-regulated by inhibitors of ERK and p38 MAPK (49). N^{ε}-(carboxymethyl) lysine (CML) is a prevalent AGE, and CML-collagen induced apoptosis in human dermal fibroblasts, while inhibitors of ROS, p38 and JNK MAPK reduced CML-collagen-induced apoptosis in fibroblasts (50, 51). These findings and our results suggest that AGEs influence DM complications via the RAGE, MAPK, and NF-κB pathways. Therefore, AGEs aggravate inflammatory responses by up-regulating IL-6 and ICAM-1 expression via the RAGE, MAKP, and NF-κB pathways in gingival fibroblasts and influence the pathogenesis of DM-associated periodontitis. The blockade of this AGE signaling pathway has potential in the treatment of DM-associated periodontitis.

Acknowledgements

This study was supported in part by Grants-in Aid for Scientific Research from the Japan Society for the Promotion of Science (25253104, 15K15701, 15K11391,

15K20621 and 16K20673). None of the authors have any conflicts of interest related to this study.

References

1. Nelson RG. Periodontal disease and NIDDM in Pima Indians. *Diabetes Care* 1990;**13**:836-840.

2. Wang TT, Chen TH, Wang PE *et al.* A population-based study on the association between type 2 diabetes and periodontal diseases in 12,123 middle-aged Taiwanese (KCIS No. 21). *J Clin Periodontol* 2009;**36**:372-379.

3. Demmer RT, Holtfreter B, Desvarieux M *et al.* The influence of type 1 and type 2 diabetes on periodontal disease progression: prospective results from the study of health in Pomerania (SHIP). *Diabetes Care* 2012;**35**:2036-2042.

4. Taylor GW, Burt BA, Becker MP, Genco RJ, Shlossman M. Glycemic control and alveolar bone loss progression in type 2 diabetes. *Ann Periodontol* 1998;**3**:30-39.

5. Khader YS, Dauod AS, El-Qaderi SS, Alkafajei A, Batayha WQ. Periodontal status of diabetics compared with nondiabetics: a meta-analysis. *J Diabetes Complications* 2006;**20**:59-68.

6. Lalla E, Lamster IB, Drury S, Fu C, Schmidt AM. Hyperglycemia, glycoxidation and receptor for advanced glycation endproducts: potential mechanisms underlying diabetic complication, including diabetes-associated periodontitis. *Periodontol 2000* 2000;**23**:50-62.

7. Taylor JJ, Preshaw PM, Lalla E. A review of the evidence for pathogenic mechanisms that may link periodontitis and diabetes. *J Periodontol* 2013;84(4 Suppl.):S113-S134.

8. Powers AC. Diabetes mellitus. In: Longo DL, Fauci AS, Kasper DL *et al.*, eds. *Hallison's Principles of Internal Medicine, 18th ed*. New York: McGraw-Hill Education, 2011:2980-2987.

9. Nathan DM. Long-term complications of diabetes mellitus. *N Engl J Med* 1993;**328**: 1676-1685.

10. Guthrow CE, Morris MA, Day JF, Thorpe SR, Baynes JW. Enhanced nonenzymatic

glycosylation of human serum albumin in diabetes mellitus. *Proc Natl Acad Sci USA* 1979;**76**:4258-4261.

11. Goldin A, Beckman JA, Schmidt AM, Creager MA. Advanced glycation end products. Sparking the development of diabetic vascular injury. *Circulation* 2006;**114**:597-605.

12. Gurav A, Jadhav V. Periodontitis and risk of diabetes mellitus. *J Diabetes* 2011;**3**:21-28.

13. Schmidt AM, Weidman E, Lalla E *et al.* Advanced glycation endproducts (AGEs) induce oxidant stress in the gingiva: A potential mechanism underlying accelerated periodontal disease associated with diabetes. *J Periodontal Res* 1996;**31**:508-515.

14. Zizzi A, Tirabassi G, Aspriello SD, Piemontese M, Rubini C, Lucarini G. Gingival advanced glycation end-products in diabetes mellitus-associated chronic periodontitis: An immunohistochemical study. *J Periodont Res* 2013;**48**:293-301.

15. Katz J, Bhattacharyya I, Farkhondeh-Kish F, Perez FM, Caudle RM, Heft MW. Expression of the receptor of advanced glycation end products in gingival tissues of type 2 diabetes patients with chronic periodontal disease: a study utilizing immunohistochemistry and RT-PCR. *J Clin Periodontol* 2005;**32**:40-44.

16. Katz J, Caudle RM, Bhattacharyya I, Stewart CM, Cohen DM. Receptor for advanced glycation end product (RAGE) upregulation in human gingival fibroblasts incubated with nornicotine. *J Periodontol* 2005;**76**:1171-1174.

17. Ren L, Fu Y, Deng Y, Qi L, Jin L. Advanced glycation end products inhibit the expression of collagens type I and III by human gingival fibroblasts. *J Periodontol* 2009;**80**:1166-1173.

18. Yu S, Li H, Ma Y, Fu Y. Matrix metalloproteinase-1 of gingival fibroblasts influenced by advanced glycation end products (AGEs) and their association with receptor for AGEs and nuclear factor-kB in gingival connective tissue. *J Periodontol* 2012;**83**:119-126.

19. Sakamoto E, Mihara C, Ikuta T, Inagaki Y, Kido J, Nagata T. Inhibitory effects of advanced glycation end-products and *Porphyromonas gingivalis* lipopolysaccharide on the expression of osteoblastic markers of rat bone marrow cells in culture. *J Periodontal Res* 2016;**51**:313-320.

20. Kishimoto T. The biology of interleukin-6. *Blood* 1989;**74**:1-10.

21. Duarte PM, de Oliveira MC, Tambeli CH, Parada CA, Casati MZ, Nociti FH Jr. Overexpression of interleukin-1beta and interleukin-6 may play an important role in periodontal breakdown in type 2 diabetic patients. *J Periodontal Res* 2007;**42**:377-381.

22. Mesia R, Gholami F, Huang H *et al.* Systemic inflammatory responses in patients with type 2 diabetes with chronic periodontitis. *BMJ Open Diabetes Res Care* 2016;**4**:e000260.

23. Chiu H-C, Fu M M-J, Yang T-S *et al.* Effect of high glucose, *Porphyromonas gingivalis* lipopolysaccharide and advanced glycation end-products on production of interleukin-6/-8 by gingival fibroblasts. *J Periodontal Res* 2017;**52**:268-276.

24. Hubbard AK, Rothlein R. Intercellular adhesion molecule-1 (ICAM-1) expression and cell signaling cascades. *Free Radic Biol Med* 2000;**28**:1379-1386.

25. Witkowska AM, Borawska MH. Soluble intercellular adhesion molecule-1 (sICAM-1): an overview. *Eur Cytokine Netw* 2004;**15**:91-98.

26. Teijeira A, Hunter MC, Russo E *et al.* T cell migration from inflamed skin to draining lymph nodes requires intralymphatic crawling supported by ICAM-1/LFA-1 interactions. *Cell Rep* 2017;**18**:857-865.

27. Chen H-T, Tsou H-K, Chen J-C, Shih J M-K, Chen Y-J, Tang C-H. Adiponectin enhances intercellular adhesion molecule-1 expression and promotes monocyte adhesion in human synovial fibroblasts. PLoS One 2014;**9**:e92741.

28. Liu J, Duan J, Wang Y, Ouyang X. Intracellular adhesion molecule-1 is regulated by Porphyromonas gingivalis through nucleotide binding oligomerization domain-containing proteins 1 and 2 molecules in periodontal fibroblasts. *J Periodontol*

2014;**85**:358-368.

29. Zhang D, Zheng H, Zhao J *et al. Porphorymonas gingivalis* induces intracellular adhesion molecule-1 expression in endothelial cells through the nuclear factor-kappa B pathway, but not through the p38 MAPK pathway. *J Periodontal Res* 2011;**46**:31-38.

30. Miyagawa T, Fujita T, Ouhara K *et al.* Irsogladine maleate regulates the inflammatory related genes in human gingival epithelial cells stimulated by *Aggregatibacter actinomycetemcomitans*. *Int Immunopharmacol* 2013;**15**:340-347.

31. Abu Seman N, Anderstam B, Wan Mohamud WM, Östenson CG, Brismar K, Gu HF. Genetic, epigenetic and protein analyses of intercellular adhesion molecule Malaysian subjects with type 2 diabetes and diabetic nephropathy. *J Diabetes Complications* 2015;**29**:1234-1239.

32. Matsui T, Nakamura N, Ojima A, Nishino Y, Yamagishi SI. Sulforaphane reduces advanced glycation end products (AGEs)-induced inflammation in endothelial cells and rat aorta. *Nutr Metab Cardiovasc Dis* 2016;**26**:797-807.

33. Takeuchi M, Makita Z, Bucala R, Suzuki T, Koike T, Kameda Y. Immunological evidence that non-carboxymethyllysine advanced glycation end-products are produced from short chain sugars and dicarbonyl compounds in vivo. *Mol Med* 2000;**6**:114-125.

34. Okada H, Murakami S. Cytokine expression in periodontal health and disease. *Crit Rev Oral Biol* 1998;**9**:248-266.

35. Mogi M, Otogoto J, Ota N, Inagaki H, Minami M, Kojima K. Interleukin 1 beta, interleukin 6, beta 2-microglobulin, and transforming growth factor-alpha in gingival crevicular fluid from human periodontal disease. *Arch Oral Biol* 1999;**44**:535-539.

36. Sawada S, Chosa N, Ishisaki A, Naruishi K. Enhancement of gingival inflammation induced by synergism of IL-1β and IL-6. *Biomed Res* 2013;**34**:31-40.

37. Sundararaji KP, Samuvel DJ, Li Y, Sanders JJ, Lopes-Virella MF, Huang Y. Interleukin-6 released from fibroblasts is essential for up-regulation of matrix metalloproteinase-1 expression by U937 macrophages in coculture: cross-talking

between fibroblasts and U937 macrophages exposed to high glucose. *J Biol Chem* 2009;**284**:13714-13724.

38. Blair HC, Athanasou NA. Recent advances in osteoclast biology and pathological bone resorption. *Histol Histopathol* 2004;**19**:189-199.

39. Asai A, Okajima F, Nakagawa K *et al.* Phosphatidylcholine hydroperoxide-induced THP-1 cell adhesion to intracellular adhesion molecule-1. *J Lipid Res* 2009; **50**:957-965.

40. Ikeda M, Ikeda U, Shimada K, Minoa S, Kano S. Regulation of ICAM-1 expression by inflammatory cytokines in rat mesangial cells. *Cytokine* 1996;**8**:109-114.

41. Wang L, Walia B, Evans J, Gewirtz AT, Merlin D, Sitaraman SV. IL-6 induces NF-kappa B activation in the intestinal epithelia. *I Immunol* 2003;**171**:3194-3201.

42. Suzuki, Hashizume M, Yoshida H, Shiina M, Mihara M. Intercellular adhesion molecule-1 on synovial cells attenuated interleukin-6-induced inhibition of osteoclastogenesis induced by receptor activator for nuclear factor κB ligand. *Clin Exp Immunol* 2011;**163**:88-95.

43. Waddington RJ, Moseley R, Embery G. Reactive oxygen species: a potential role in the pathogenesis of periodontal diseases. *Oral Dis* 2000;**6**:138-151.

44. Ohnishi T, Bandow K, Kakimoto K, Machigashira M, Matsuyama T, Matsuguchi T. Oxidative stress causes alveolar bone loss in metabolic syndrome model mice with type 2 diabetes. *J Periodontal Res* 2009;**44**:43-51.

45. Berrou J, Tostivint I, Verrecchia F *et al.* Advanced glycation end products regulate extracellular matrix protein and protease expression by human glomerular mesangial cells. *Int J Mol Med* 2009;**23**:513-520.

46. Chen SC, Guh JY, Hwang CC *et al.* Advanced glycation end-products activate extracellular signal-regulated kinase via the oxidative stress-EGF receptor pathway in renal fibroblasts. *J Cell Biochem* 2010;**109**:38-48.

47. Abbass MM, Korany NS, Salama AH, Dmytryk JJ, Safiejko-Mroczka B. The relationship between receptor for advanced glycation end products expression and the severity of periodontal disease in the gingiva of diabetic and non diabetic periodontitis patients. *Arch Oral Biol* 2012;**57**:1342-1354.

48. Liu Y, Liang C, Liu X *et al.* AGEs increased migration and inflammatory responses of adventitial fibroblasts via RAGE, MAPK and NF-kappa B pathways. *Atherosclerosis* 2010;**208**:34-42.

49. Tang M, Zhong M, Shang Y *et al.* Differential regulation of collagen types I and III expression in cardiac fibroblasts by AGEs through TRB3/MAPK signaling pathway. *Cell Mol Life Sci* 2008;**65**:2924-2932.

50. Alikhani M, Maclellan CM, Raptis M, Vora S, Trackman PC, Graves DT. Advanced glycation end products induce apoptosis in fibroblasts through activation of ROS, MAP kinases, and the FOXO1 transcription factor. *Am J Physiol Cell Physiol* 2007;**292**:C850-C856.

51. Singh R, Barden A, Mori T, Beilin L. Advanced glycation end-products: a review. *Diabetologia* 2001;**44**:129-146.

Figure legends

Figure 1. Effects of AGEs on cell viability and morphology of HGFs

(A) HGFs were seeded at 4800 cells/cm^2, cultured for five days, and then treated with fresh BSA (500 μg/ml; open column) and AGEs (500 μg/ml; closed column) every day for 24-96 h. Cell proliferation activity was assessed using Cell Counting Kit-8®. Data are expressed as the mean±SD of three independent experiments (** P<0.01). (B) Cultured HGFs were observed by phase-contrast microscopy after a culture with or without BSA (500 μg/ml) and AGEs (500 μg/ml) for 72 h. (Magnification x 40).

Figure 2. Effects of AGEs on the gene expression of RAGE and inflammation-related factors in HGFs

(A) Sub-confluent HGFs were cultured with BSA (500 μg/ml) and AGEs (500 μg/ml) for 24, 48, and 72h. Isolated RNAs were analyzed by RT-PCR using specific primers for *RAGE*, *IL6*, *ICAM1*, *MCP1*, *VEGF,* and *GAPDH* (Table 1). (B) RNA samples were isolated from HGFs treated with BSA (0-1000 μg/ml; open column) and AGEs (50-1000 μg/ml; closed column) for 48 h and *IL6* mRNA expression was analyzed by qRT-PCR. (C) *ICAM1* mRNA expression in HGFs treated with BSA (500 μg/ml; open column) and AGEs (500 μg/ml; closed column) for 48 h was assessed by qRT-PCR.

mRNA expression was normalized to that of *GAPDH*. Data are expressed as the mean ±SD of three independent experiments (* $P<0.05$, ** $P<0.01$).

Figure 3. Effects of AGEs on the productions of RAGE, IL-6, and ICAM-1 and ROS activity in HGFs

(A) Sub-confluent HGFs were treated with BSA (500 μg/ml) and AGEs (500 μg/ml) for 24 h. Cell lysates were analyzed by Western blotting using a RAGE antibody as described in the Materials and Methods. The results obtained show a representative of three independent experiments. (B, C) Sub-confluent HGFs were treated with BSA (500 μg/ml; open column) and AGEs (500 μg/ml; closed column) for 48 h. The amounts of IL-6 (B) in the supernatant and ICAM-1 (C) in the cell lysate were measured using each ELISA as described in the Materials and Methods. The production of ICAM-1 was normalized to the total cell protein amount. (D) ROS activity in HGFs treated with BSA (500 μg/ml; open diamond) and AGEs (500 μg/ml; closed square) for 6-72 h was assessed using a ROS activity assay kit. Data are expressed as the mean±SD of three independent experiments (** $P<0.01$).

Figure 4. Effects of rhIL-6 on ICAM-1 expression and inhibitory effects of

RAGE and IL-6 siRNAs on AGE-induced *IL6* and *ICAM1* mRNA expression in HGFs

Sub-confluent HGFs were treated with rhIL-6 (50 ng/ml) for 24 h and 48 h. (A) RNA was isolated from the treated cells and the mRNA expression of *ICAM1* was assayed by qRT-PCR. The mRNA expressions of *ICAM1* was normalized to that of *GAPDH*. (B) The amount of ICAM-1 in the lysate of treated cells was measured using ELISA as described in the Materials and Methods. The production of ICAM-1 was normalized to the total cell protein concentration.

HGFs were seeded at 9500 cells/cm^2, cultured for one day, reached 70% confluency, and then treated with control siRNA (siCont.; 10μM), RAGE siRNA (siRAGE; 10 μM), or IL-6 siRNA (siIL6; 10μM) for 24 h as described in the Materials and Methods. HGFs were cultured further with BSA (500 μg/ml; open column) and AGEs (500 μg/ml; closed column) for 48 h. RNA samples in cells transfected with each siRNA were isolated, the expression of RAGE mRNA was analyzed by RT-PCR (C), and the mRNA expression of *IL6* (D and F) and *ICAM1* (E and G) was assessed by qRT-PCR. The mRNA expression of *IL6* and *ICAM1* was normalized to that of *GAPDH*. Data are expressed as the mean±SD of three independent experiments (* $P<0.05$, ** $P<0.01$).

Figure 5. Effects of MAPK inhibitors on AGE-induced IL-6 and ICAM-1 expression and phosphorylation of MAPK in HGFs

(A) Sub-confluent HGFs were treated with 500 μg/ml BSA and AGEs for 30min, and the cell lysate were collected. MAPK phosphorylation in the treated cell lysates was analyzed by Western blotting using antibodies against p38, phospho-p38, ERK, phospho-ERK, JNK, and phospho-JNK. (B-E) Sub-confluent HGFs were pretreated with SB2013580 (30 μM), U0126 (10 μM), and SP600125 (10 μM) for 2 h and then cultured with BSA (500 μg/ml; open column) or AGEs (500 μg/ml; closed column) for 24 h. The mRNA expression of *IL6* (B) and *ICAM1* (C) was assayed by qRT-PCR. mRNA expression was normalized to that of *GAPDH*. After the culture with BSA (open column) and AGEs (closed column) for 48 h, the amounts of IL-6 in the supernatant (D) and ICAM-1 in the cell lysate (E) were measured using each ELISA kit. Data are expressed as the mean±SD of three independent experiments (* $P<0.05$, ** $P<0.01$).

Figure 6. Effects of the NF-κB inhibitor on AGE-induced IL-6 and ICAM-1 expression and phosphorylation of p65 and IkBα in HGFs

(A) Sub-confluent HGFs were treated with 500 μg/ml BSA and AGEs for 30 min, and the cell lysate was collected. NF-κB phosphorylation was analyzed by Western blotting using antibodies against p65, phospho-p65, IκBα, and phospho-IκBα. (B-E) Sub-confluent HGFs were pretreated with an IKK inhibitor; Bay11-7082 (50 μM) for 24 h, and then cultured with BSA (500 μg/ml; open column) and AGEs (500 μg/ml; closed column) for 24 h. RNA samples were isolated from the treated cells and the mRNA expression of *IL6* (B) and *ICAM1* (C) was measured by qRT-PCR. The mRNA expression of *IL6* and *ICAM1* was normalized to that of *GAPDH*. The supernatant and cell lysate were prepared from HGFs pre-cultured with Bay11-7082 (50 μM) for 24 h and then cultured with BSA (500 μg/ml; open column) and AGEs (500 μg/ml; closed column) for 48 h, and the amounts of IL-6 in the supernatant (D) and ICAM-1 in the cell lysates (E) were measured using each ELISA kit. Data are expressed as the mean ±SD of three independent experiments (* $P<0.05$, ** $P<0.01$).

Figure 7. Effects of AGEs on THP-1 cell adhesion to HGFs and inhibitory effects of IL-6 siRNA on AGE-induced cell adhesion

(A) Sub-confluent HGFs were cultured with AGEs (500 μg/ml) and BSA (500 μg/ml) for 48 h and then co-cultured with THP-1 cells (1.5 x 10^6 cells/ml) labeled with a

fluorescent reagent for 30 min. THP-1 cells that adhered to HGFs were observed using an inverted fluorescence microscopy. Magnification 40x. (B) The fluorescence intensity of labelled THP-1 cells that adhered to HGFs was determined using a fluorescence microplate reader at Ex/Em=490/520 nm. Cell adhesive activity was normalized to that of untreated HGFs (Cont.). (C) In transfection experiments, THP-1 cells (1.5×10^4 cells/ml) were labeled with a fluorescent reagent and co-cultured with HGFs transfected with IL-6 siRNA (10 μM) for 30 min, and fluorescence intensity was determined using a fluorescence microplate reader. Cell adhesive activity was normalized to that of HGFs treated with BSA (BSA cont.). Data are expressed as the mean±SD of four independent cell samples (* $P<0.05$, ** $P<0.01$).

Table 1 Primers used in RT-PCR and quantitative real-time PCR

Gene	Primer
GAPDH	For: 5'-ACC ACA GTC CAT GCC ATC AT-3' Rev: 5'-TCC ACC ACC CTG TTG CTG TA-3'
GAPDH [a]	For: 5'-GAC CCC TTC ATT GAC CTC AAC TAC-3' Rev: 5'-AGC CTT CTC CAT GGT GGT GAA GAC-3'
ICAM1	For: 5'-CGT GCC GCA CTG AAC TGG AC-3' Rev: 5'-CCT CAC ACTTCA CTG TCA CCT-3'
ICAM1 [a]	For: 5'-CAA GGC CTC AGT CAG TGT GA-3' Rev: 5'-CCT CTG GCT TCG TCA GAA TC-3'
IL-6	For: 5'-ATG AAC TCC TTC TCC ACA AGC GC-3' Rev: 5'-GAA GAG CCC TCA GGC TGG ACT G-3'
IL-6 [a]	For: 5'-AGG GCT CTT CGG CAA ATG T-3' Rev: 5'-GAA GAA GGA ATG CCC ATT AAC AAC-3'
MCP-1	For: 5'-GCT CAT AGC AGC CAC CTT CAT TC-3' Rev: 5'-TGC AGA TTC TTG GGT TGT GGA G-3'
RAGE	For: 5'-GCT GTC AGC ATC AGC ATC AT-3' Rev: 5'-ATT CAG TTC TGC ACG CTC CT-3'
VEGF	For: 5'-CCA TGA ACT TTC TGC TGT CTT-3' Rev: 5'-ATC GCA TCA GGG GCA CAC AG-3'

[a] Primer for real-time PCR

Table1

90x90mm (600 x 600 DPI)

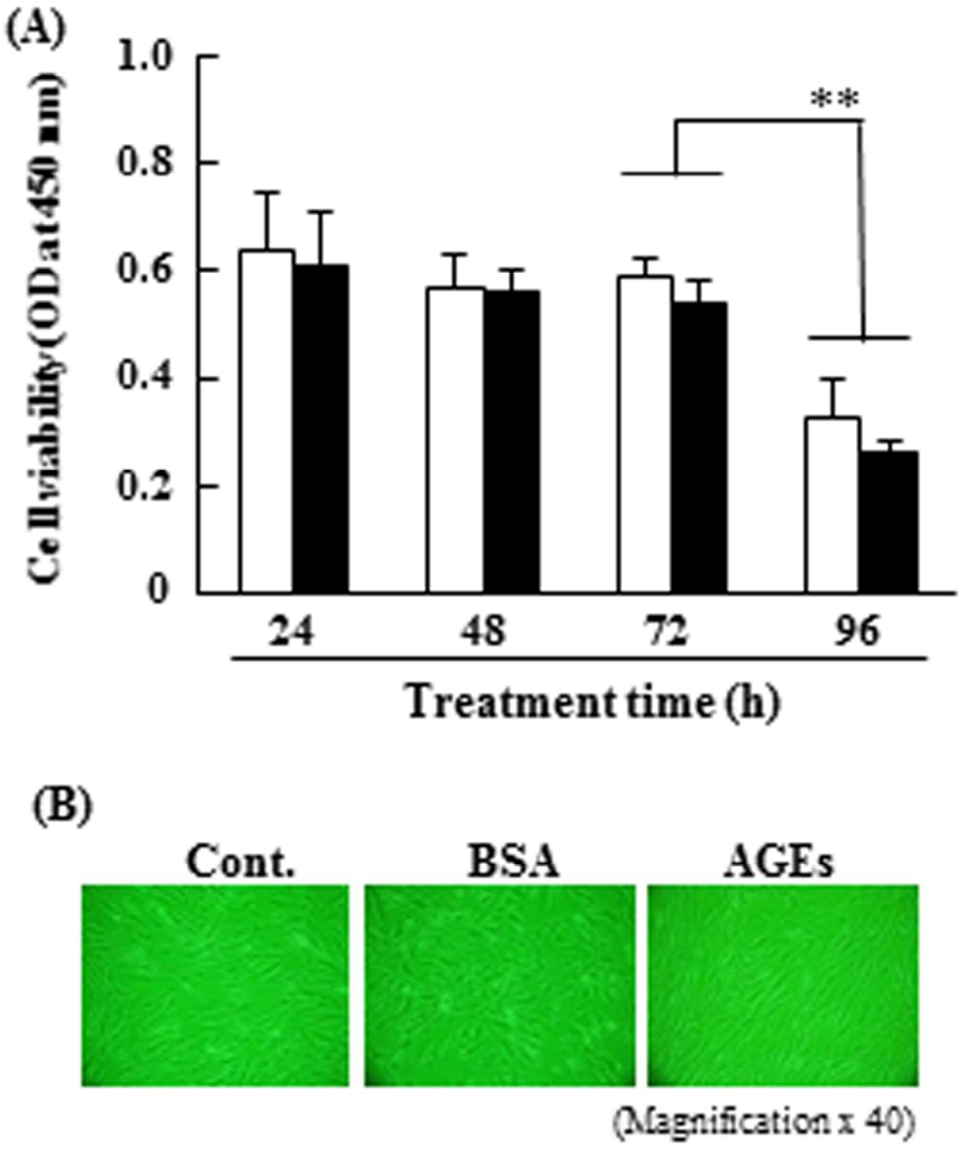

fig1

82x97mm (600 x 600 DPI)

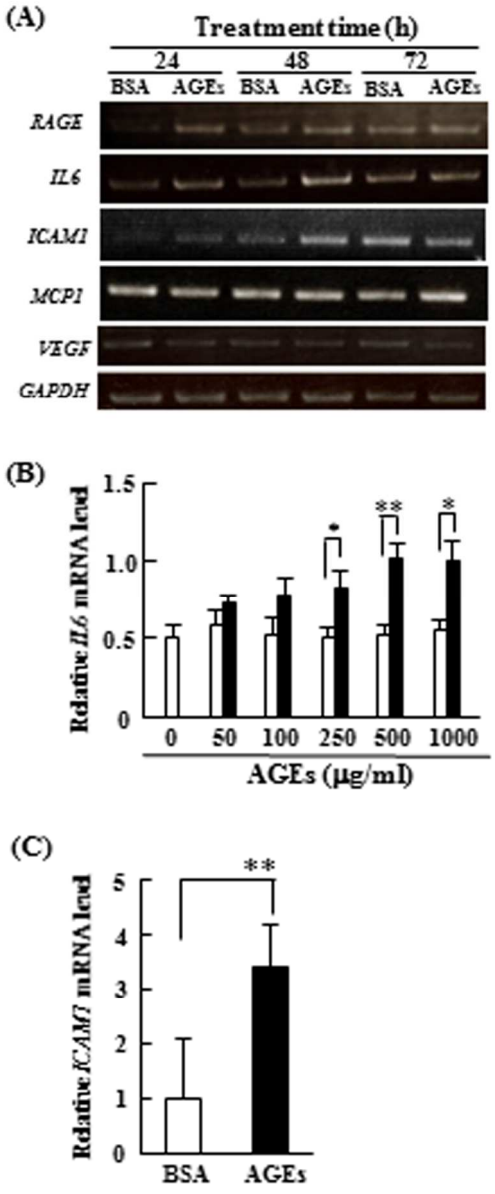

fig2

173x402mm (600 x 600 DPI)

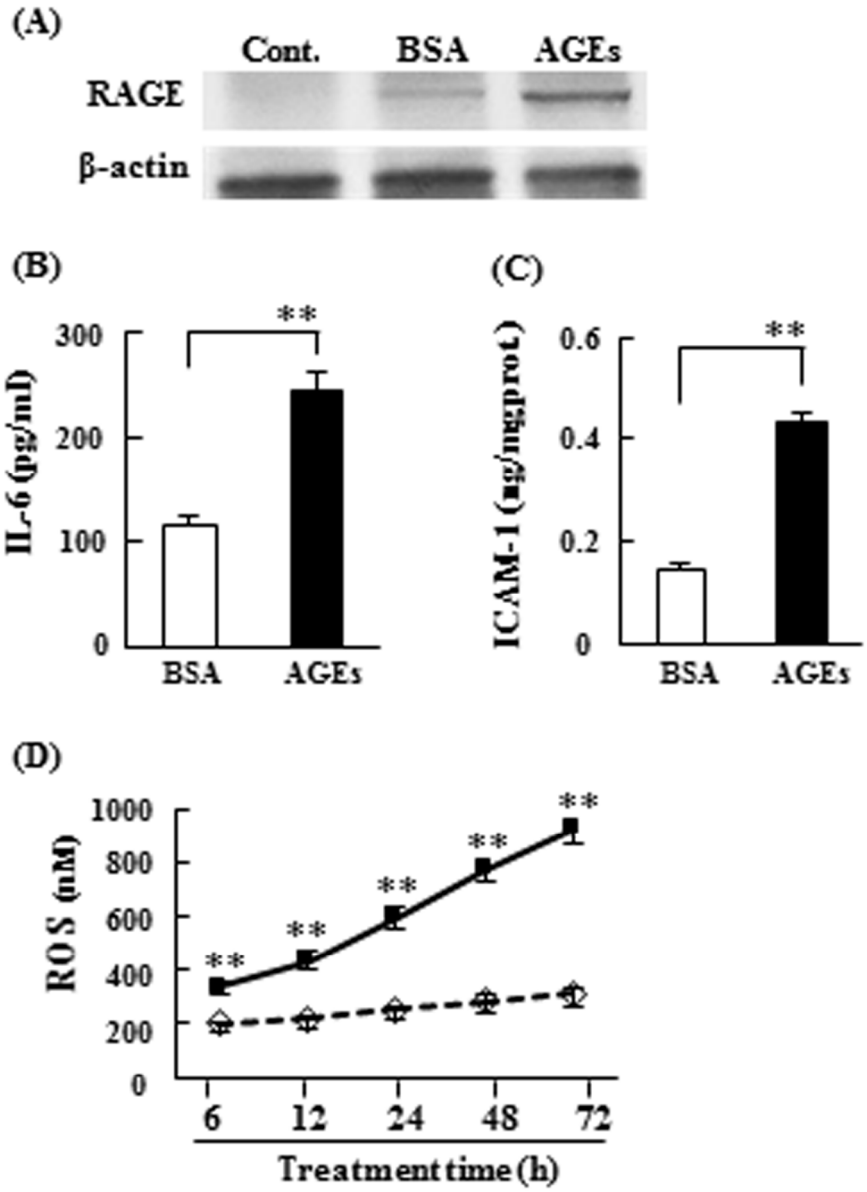

fig3

115x156mm (600 x 600 DPI)

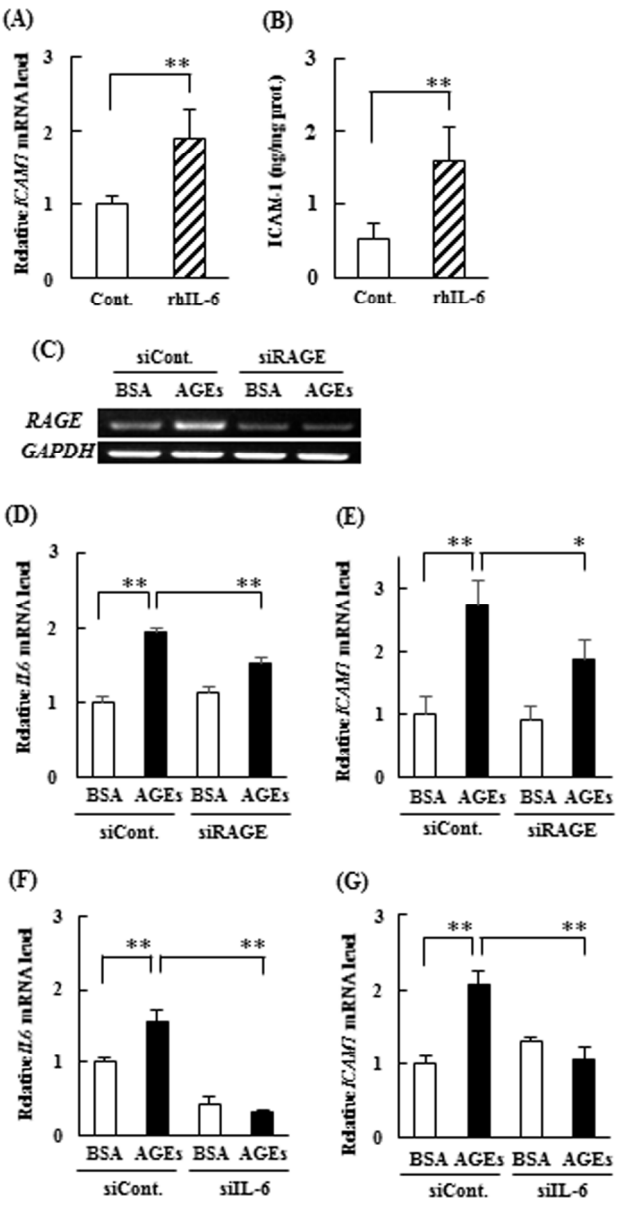

fig4

152x291mm (600 x 600 DPI)

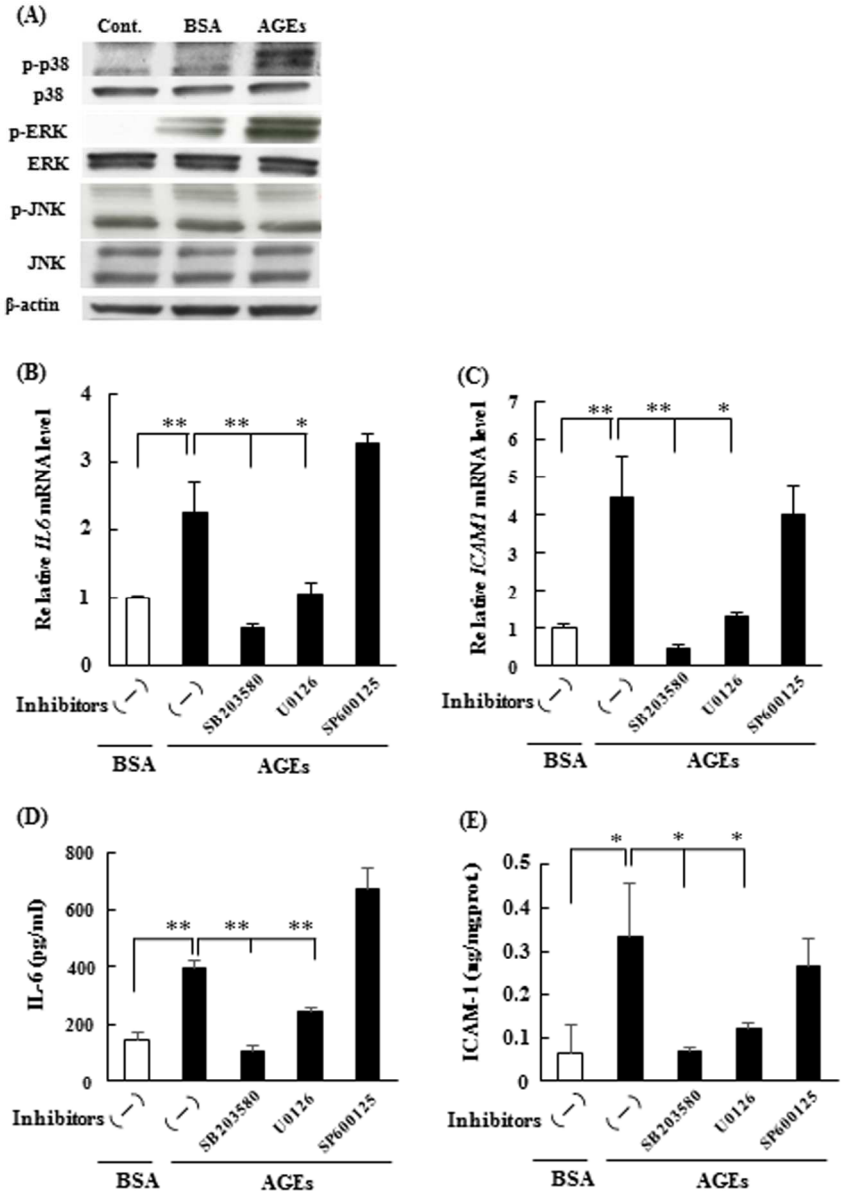

fig5

127x179mm (600 x 600 DPI)

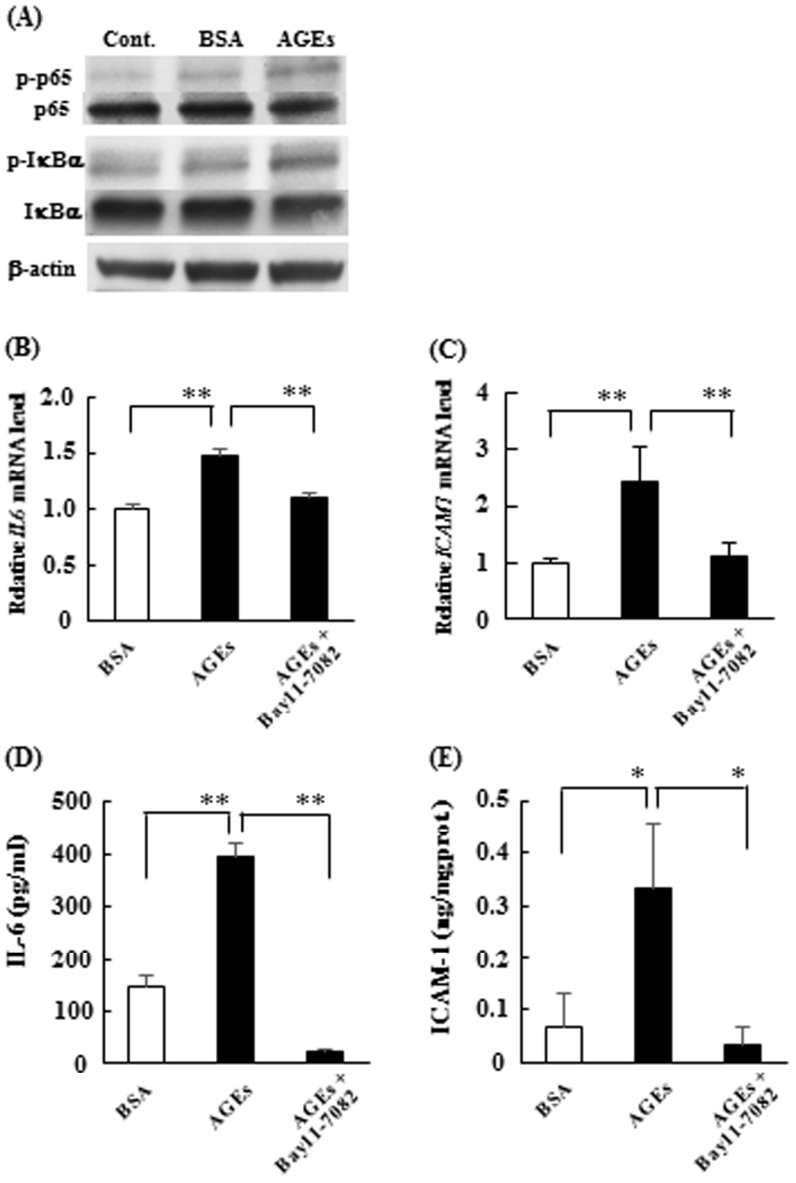

fig6

132x194mm (600 x 600 DPI)

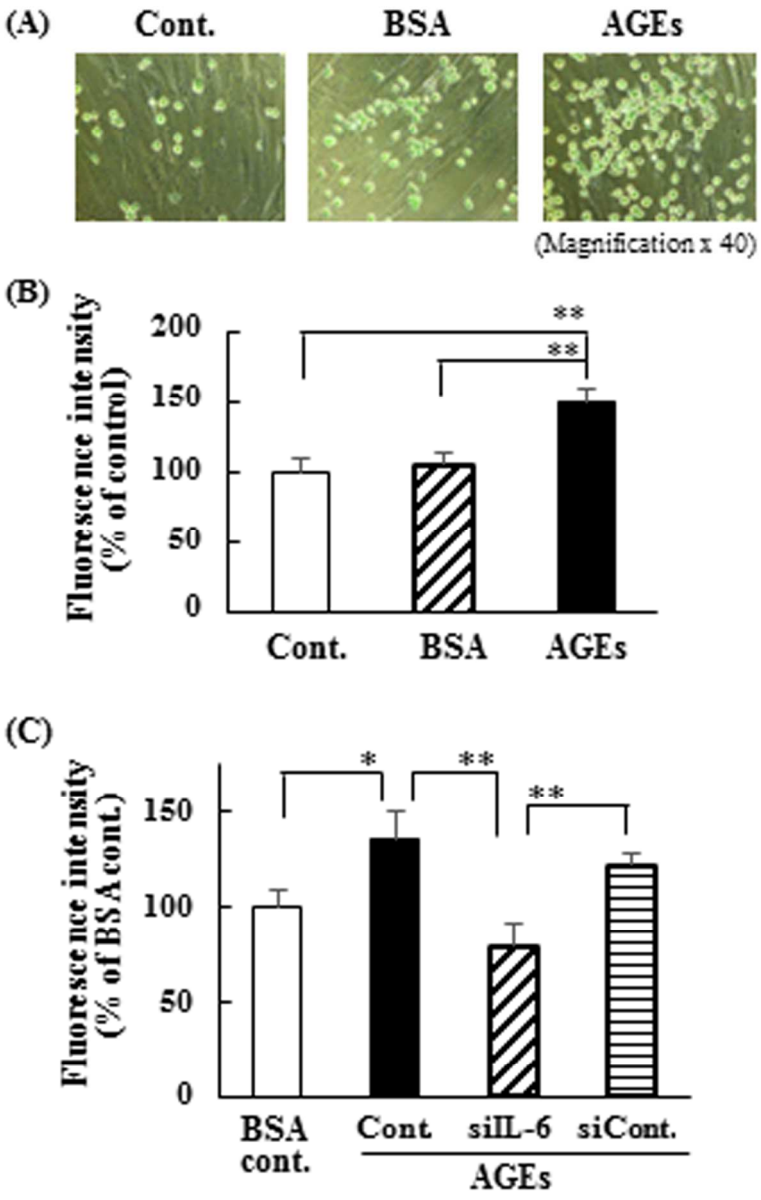

fig7

116x180mm (600 x 600 DPI)